Peer-reviewed version available at Int. J. Mol. Sci. 2019, 20, 3012; doi:10.3390/ijms20123012

FRONT MATTER

Melanopsin+RGCs are fully resistant to NMDA-induced excitotoxicity.

Running title: m+RGCs Long-term effects of NMDA-induced excitotoxicity.

AUTHOR LIST AND AFFILIATIONS:

Beatriz Vidal-Villegas*[1], Johnny Di Pierdomenico*[1], Juan A Miralles de Imperial-Ollero[1], Arturo Ortín-Martínez[1,3], Francisco M Nadal-Nicolás[1,4], Jose M Bernal-Garro[1], Nicolás Cuenca Navarro[2], Maria P Villegas-Pérez[1], Manuel Vidal-Sanz[1].**

[1] Department of Ophthalmology, University of Murcia and Instituto Murciano de Investigación Biosanitaria (IMIB)-Virgen de la Arrixaca, Murcia, Spain.
[2] Department of Physiology, Genetics and Microbiology and Multidisciplinary Institute for Environmental Studies "Ramón Margalef", University of Alicante, Alicante, Spain.
[3] Present address: Donald K Johnson Eye Institute, Krembil Research Institute, University Health Network, Ontario, Canada.
[4] Present address: Retinal Neurophysiology Section, John Edward Porter Neuroscience Research Center, National Eye Institute, National Institutes of Health, Bethesda, MD 20892, USA.

*Joint first authors
** Correspondence: manuel.vidal@um.es

Abstract

We studied short- and long-term effects of intravitreal injection of N-methyl-D-aspartate (NMDA) on melanopsin-containing (m+) and non-melanopsin-containing (Brn3a+) retinal ganglion cells (RGCs). In adult SD-rats, the left eye received a single intravitreal injection of 5µL of 100nM NMDA. At 3 and 15 months, retinal thickness was measured *in vivo* using SD-OCT. Ex vivo analyses were done at 3, 7, 14 days or 15 months after damage. Whole-mounted retinas were immunolabelled for Brn3a and melanopsin, the total number of Brn3a+RGCs and m+RGCs were quantified and their topography represented. In control retinas, the mean total numbers of Brn3a+RGCs and m+RGCs were 78,903±3,572 and 2,358±144 (mean ± SD; n=10), respectively. In the NMDA injected retinas, Brn3a+RGCs numbers diminished to 50% and 25%, at 3 and 14 days, respectively, but there was no further loss up to 15 months. The number of immunoidentified m+RGCs decreased significantly at 3 days, recovered between 3-7 days and was back to normal thereafter. OCT measurements revealed a significant thinning of the left retinas at 3 and 15 months. Intravitreal injections of NMDA induce a rapid loss of 75% of Brn3a+RGCs, a transient downregulation of melanopsin expression but not m+RGC death, and a thinning of the inner retinal layers.

Key words
NMDA, excitotoxicity, Glaucoma, melanopsin-RGCs, intrinsically photosensitive-RGCs, Brn3a+RGCs, adult albino rat, retina, SD-OCT.

Research Manuscript Sections:

Introduction

Light is converted by photoreceptors (rods and cones) into electrical signals which are initially processed at the outer synaptic layer of the retina where photoreceptor information is modulated by horizontal cells and conveyed onto bipolar cells. Signals are further processed at the inner synaptic layer where the bipolar information is modulated by amacrine cells and finally passed on to retinal ganglion cells (RGCs) in the innermost retinal layer. RGCs, the only ones whose axon leaves the retina, convey the information processed in the retina to the retinorecipient nuclei of the brain. This projection obtains relevant information from our visual world from the retina and provides it to the brain to produce image-forming as well as nonimage-forming visual functions. Retinal information that produces image-forming visual functions is carried out by the general population of RGCs that have in common the expression of Brn3a, while the information necessary to produce nonimage-forming visual functions is carried out by a small subpopulation of RGCs that express the photopigment melanopsin (m$^+$RGCs) rendering them intrinsically photosensitive (ipRGCs); the so called third photoreceptor cell-type of the retina [1].

In adult rodents, RGCs constitute less than 1% of all retinal cells [2-4]. Based on their morphology (soma size and dendritic arborization), extension of their dentritic arborization into the inner synaptic layer, electrophysiological responses to light stimulus within their receptive field, target region of the brain and genetic background it has been proposed that the rodent retina may have up to 40 different types of RGCs [5-8]. In the rat it has been estimated that excluding endothelial cells, the GCL is composed of approximately 50% displaced amacrine cells (ACs), 10% glial cells, and 40% RGCs [9]. Displaced ACs not only share their location in the retina with RGCs but overlap in size thus making it difficult to distinguish RGCs from ACs, and this has obliged the use of retrogradely transported neuronal tracers [10,11] or neuronal markers to identify RGCs. There are several markers that identify large proportions of RGCS (pan-markers) or many RGC types, including Thy-1 [12], Brn3a [13,14], RBPMS [15], class III beta-tubulin [16], Neuronal Nuclei (NeuN) [17] and Microtubule-associated protein 1A (MAP 1A) [7,18]. In addition, there are several markers that allow to identify specific types of RGCs, such as melanopsin [19] and others [7,8,20]. However, after retinal injury, many of the physiological and morphological attributes of RGCs, including their dendritic arborization may change [8,21,22], and the molecular markers may be downregulated, rendering the identification of RGCs difficult [23-28].

The characterization of the expression of Brn3a by rodent RGCs has allowed identification of the main population of RGCs that convey image-forming visual information to the brain, which represents approximately 96% of the RGC population [14]. Nonimage-forming visual behaviours depend on intrinsically photosensitive RGCs (ipRGCs), one type of RGC with a large dendritic arbor that contains the photopigment melanopsin (m$^+$RGCs), responsible for the circadian photoentrainment, pupillary reflexes and the regulation of pineal melatonin secretion [1,29,30]. Six subtypes of ipRGCs have been described to express at least small amounts of melanopsin (also known as Opn4), and are named M1-M6 [31,32]. Antibodies against melanopsin allow the identification of the large majority of ipRGCs, preferentially M1-M3, because M4, which corresponds to the ON αRGC subtype [33,34], M5 [35] and M6 [32] express less Opn4 than M1-M3 and are difficult to identify with standard immunohistochemistry [31,32,36-39]. In rats, the population of m$^+$RGCs constitute approximately 2.5 and 2.7% of the RGC population for pigmented and albino, respectively [13,14,19]. Moreover, because Brn3a and melanopsin are hardly-ever expressed in the same RGC, immunohistofluorescent studies using these two markers together allows the study, in parallel but independently, of the responses of these two types of RGCs to different retinal injuries [28,40].

Glutamate excitotoxicity may be induced by the intravitreal injection of N-methyl D-Aspartate (NMDA) which results in the excessive stimulation of NMDA receptors, one of the three ionotropic glutamate receptor subtypes widely expressed by inner retinal neurons. Glutamate excitotoxicity is thought to play an important role in the loss of RGCs in various retinal injuries [41,42] including glaucoma [43-47], transient ischemia [48] and optic nerve injury [49,50], and may also play a key role

in many CNS diseases involving neuronal death [51]. Excessive NMDA receptor stimulation may result in alterations of the Na^+/K^+ homeostasis, excessive influx of large amounts of Ca^{2+} into the cell [52] which may result in direct damage by activation of enzymes that damage DNA and cell membranes [53] and by the induction of apoptosis through activation of c-AMP [54]. Animal models of NMDA-induced retinal excitotoxicity are often used to explore molecular mechanisms of RGC apoptosis and its protection [55-63].

The susceptibility of RGCs to NMDA-mediated excitotoxicity has been studied previously in adult rats [55,59] and mice [56,64], as well as the effects of intravitreal NMDA on the specific type population of m^+RGCs [56,64]. However, these were short term studies spanning up to 58 days after NMDA injection and thus the short- and long-term effects of NMDA excitotoxicity on the population of RGCs expressing Brn3a had not been investigated so far. Moreover, to what extent NMDA-induced neurotoxicity may result in long term effects on the retinal architecture and on the population of ipRGCs itself had not been previously investigated.

In the present studies we take advantage of recent techniques developed in the laboratory to identify, count and map in the same retinal wholemounts the populations of RGCs expressing Brn3a or melanopsin. Moreover, we use modern non-invasive techniques, such as the Spectral Domain Optical Coherence Tomography (SD-OCT), to image and analyse retinal thickness longitudinally at short (3months) and long (15 months) survival intervals. We investigate the responses of the general population of RGCs ($Brn3a^+$) and the population of ipRGCs (m^+RGCs) to excitotoxicity induced by the intravitreal injection of NMDA. Overall our studies indicate that the general population of $Brn3a^+$RGCs is quite sensible to NMDA mediated excitotoxicity and induces very rapidly the loss of approximately 75% of the population. In contrast, m^+RGCs after a transient downregulation of melanopsin, show a remarkable capacity for survival of the entire m^+RGC population, for periods of up to 15 months. Examination of these retinas with SD-OCT reveals that NMDA-injected retinas showed an important reduction in the thickness of the total and inner retina that was present at 3 months and progressed up to 15 months. Short accounts of this work have been published in abstract format [65].

Results

We have included in this study a total of 51 rats whose left eye received an intraocular injection of 5 µl NMDA (100nM). The first 28 were analysed within the first 14 days after the injection while the remaining 23 were analysed at 15 months to investigate the long-term effects of the excitotoxic insult on the survival of two RGC populations, the $Brn3a^+$RGCs and the m^+RGCs. Five additional naïve rats were used as controls. In addition, SD-OCT was used to measure retinal thickness in both retinas of each animal at 3 and 15 months after NMDA injection.

Rapid and massive loss of $Brn3a^+$RGCs shortly after NMDA injection.

When the right and naïve retinas or the vehicle injected retinas, were examined under the fluorescence microscope, $Brn3a^+$RGCs showed the typical distribution throughout the entire retina with higher densities on the superior retina, just above the optic nerve along the visual streak, as described in detail before [66-68]. Changing the fluorescent filter allowed to see m^+RGCs distributed in a complementary fashion to $Brn3a^+$RGCs and, as previously shown by this Laboratory [14,19], we were not able to see any doubly immunolabelled RGC, thus confirming that these markers are exclusive to one population (Figure 1).

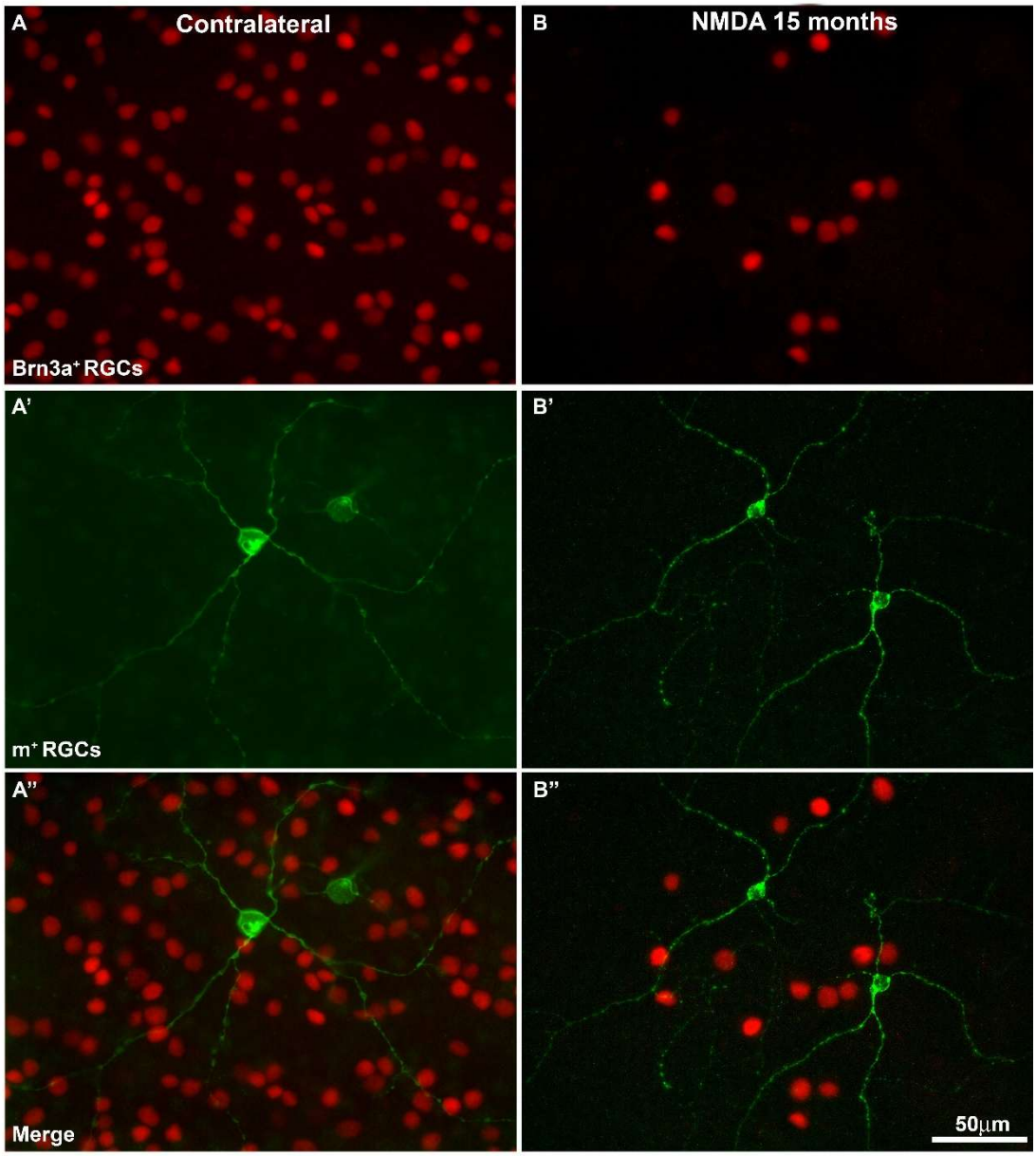

Figure 1. Magnifications from flat mounted retinas showing Brn3a⁺RGCs (A-B) and m⁺RGCs (A'-B') and both signals (merge) (A"-B") in contralateral (A-A") and NMDA-treated retinas (B-B") analyzed at 15 months after the injection. Brn3a labels cell nuclei while melanopsin allows to see cell somata as well as primary dendrites on the plane of focus. When both images are overlapped (A''-B'') one can appreciate the smaller density of m⁺RGCs compared to Brn3a⁺RGCs, as well as the fact that there are no doubly labelled RGCs. Note that 15 months after NMDA injection there are fewer Brn3a⁺RGCs. Scale bar= 50 µm.

Total numbers of Brn3a⁺RGCs (78,903±3,573 mean±SD, n=10) in the naïve retinas were comparable to those in the right fellow retinas of our experimental groups analysed at 3, 7 and 14 days (76,472±5,815 Brn3a⁺RGCs mean±SD, n=29), or 15 months (81,480±5,602 mean±SD, n=20) after NMDA injection, as well as to those obtained in previous studies from this Laboratory [13,14,19,69] (Figures 1, 2. Table 1).

The left NMDA-injected retinas showed significant decreases in the total numbers of Brn3a⁺RGCs. By 3 days after NMDA injection, the total number of Brn3a⁺RGCs was 38,940±22,443 (n=9) which is significantly smaller than naïve controls and contralateral retinas ($p \leq 0.001$, Mann Whitney test). There were further reductions at 7 (21,811±9,750 mean±SD, n=6) and 14 days (19,348±8,502 mean±SD, n=10) but these were not statistically significant when compared to 3 days, indicating that in this injury model RGC loss occurs early after NMDA injection but there is no further progression between 3 and 14 days (Figure 2, Table 1). Moreover, at 15 months, the left NMDA-injected retinas showed

significantly lower numbers than their fellow retinas (15,099±8,595 mean±SD, n=23) that corresponded to a survival of approximately 19%, although these values were not different from those obtained at 14 days (Mann Whitney test, p=0,342), indicating that there is no further loss of Brn3a⁺RGCs between 14 days and 15 months. (Figures 1, 2, 3, Table 1).

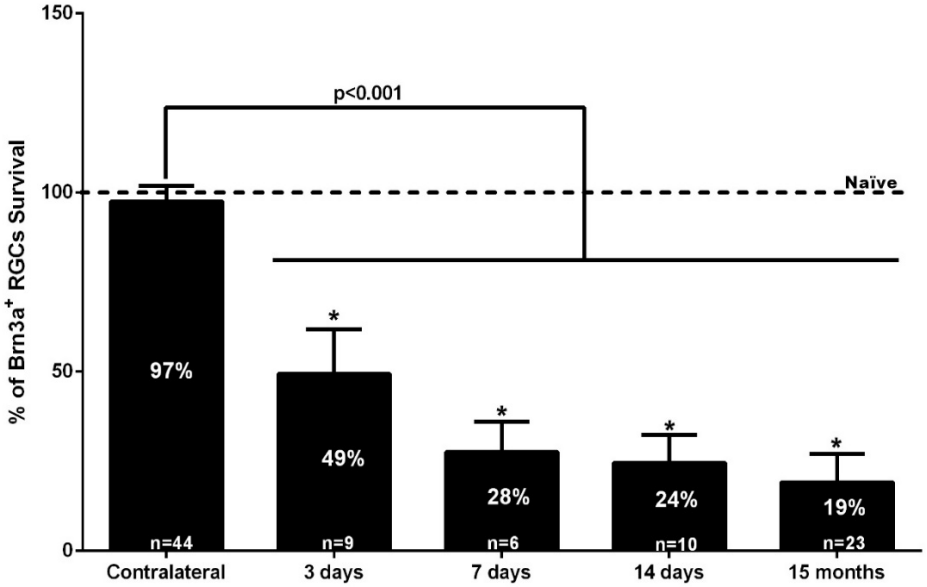

Figure 2. Bar graph showing the percent vs. intact retinas of the total numbers of Brn3a⁺RGCs ± standard deviation quantified in the contralateral uninjured and experimental retinas analyzed 3, 7, 14 days (d) or 15 months (m) after the intraocular injection of 100 nM NMDA. The number of Brn3a⁺RGCs in the intact naïve retinas was considered 100%. The number of analyzed retinas is shown at the bottom of each bar. Statistically significant differences were observed (Kruskal-Wallis test, p<0.001) between values obtained in intact retinas (Naïve) or right eye retinas (Contralateral) and retinas examined at 3, 7, 14 days or 15 months. However, no significant differences were observed (*Kruskal-Wallis test, p>0.05) between experimental groups analyzed at 3, 7, 14 days or 15 months, which suggests that NMDA-induced Brn3a⁺RGCs does not progress between 3 days and 15 months.

Retinal distribution of Brn3a⁺RGCs in the NMDA injected retinas did not adopt any particular spatial pattern, their loss was diffuse and distributed over the entire retinas (Figure. 3), although occasionally there was a smaller density in the superior temporal quadrant that could be explained by the proximity to the intraocular puncture and thus, a region exposed to a greater concentration of the injected NMDA.

After a transient downregulation of melanopsin, m⁺RGCs appear fully resistant to NMDA injection.

Total numbers of m⁺RGCs (2,358±143 mean±SD, n=10) in the naïve retinas were comparable to those obtained in the right fellow retinas of our experimental groups analysed at 3, 7 and 14 days (2,257±228 m⁺RGCs mean±SD, n=29), or at 15 months (2,166±96 mean±SD, n=9) after NMDA injection, as well as to those obtained in previous studies from this Laboratory [13,19,69] (Figures 1,3,4 Table 2).

By 3 days after intravitreal injection of NMDA, the total number of m⁺RGCs was 1,516±312 (n=10), a significant reduction when compared to naïve or contralateral retinas (p≤0.001, Kruskal Wallis test) (Figure 2). Surprisingly, the total number of m⁺RGCs at 7 or 14 days after NMDA injection was 2,105±445 (n=7) or 2,419±257 (n=11), showing a significant increase when compared to the values observed at 3 days, and reached comparable values to those of control retinas by 14 days (p>0.05 Kruskal Wallis, test). By 15 months after NMDA-injection, the left retinas showed a total number of m⁺RGCs (2,027±134 mean±SD, n=11) comparable with the data obtained in their right fellow retinas (2,166±96 mean±SD, n=9) (Mann Whitney test, p=0.518).

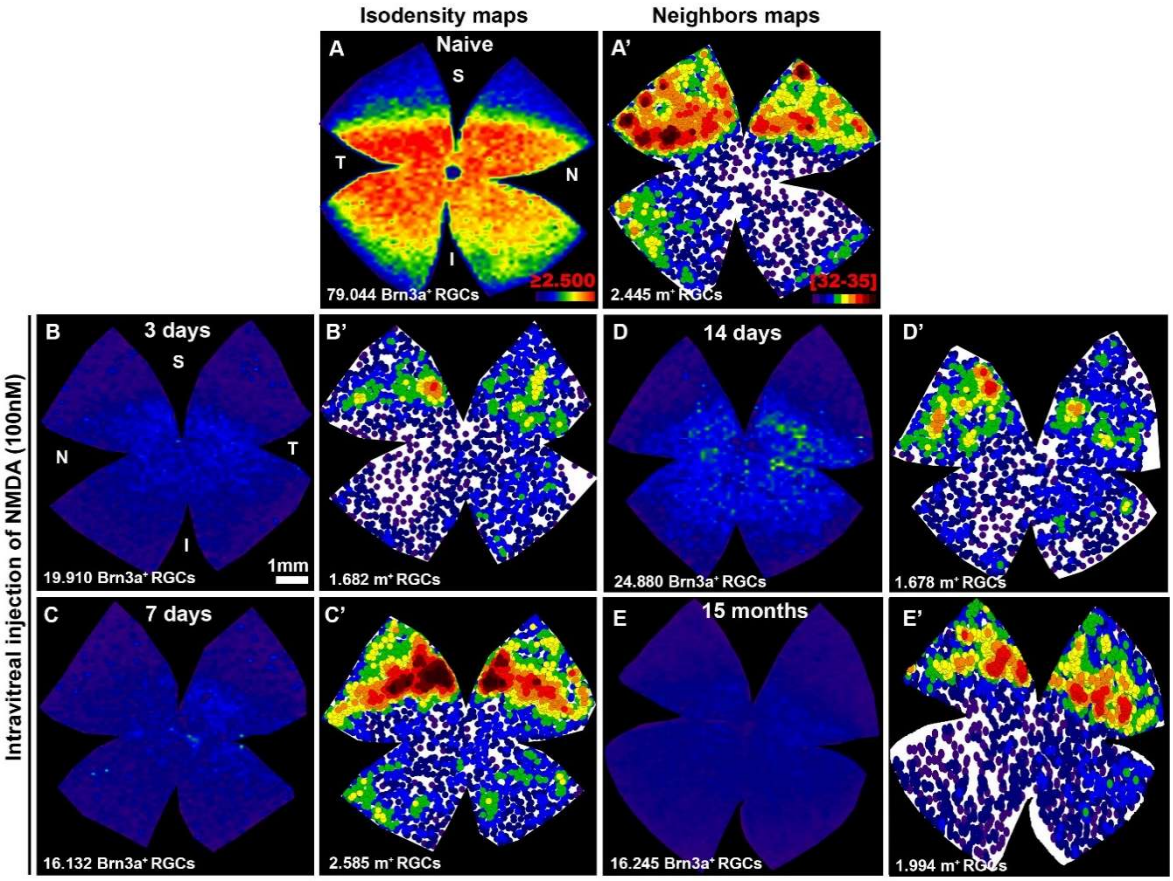

Figure 3. A-E. Isodensity maps showing the retinal topography of Brn3a⁺RGCs in intact retinas (A) or in representative retinas analyzed at 3 (B), 7 (C), 14(D) days or 15 (E) months after intravitreal injection of 100nM NMDA. A'-E'. Neighbor maps illustrating the distribution of m⁺RGCs in the same retinas shown in A-E. Isodensity maps color scale ranges from 0 (purple) to ≥ 2,500 (red) cells/mm². Neighbor map color scale, each color represents an increase of 4 neighbors in a radius of 0.0552 mm from purple (0-4 neighbors) to dark red (32-35 neighbors). Below each map is shown the total number of Brn3a⁺RGCs or m⁺RGCs counted. S: superior, I: inferior, N: nasal, T: temporal. Scale bar= 1mm

We interpret this abrupt decrease and subsequent recovery of the total number of m⁺RGCs as a transient downregulation of melanopsin, shortly after intravitreal injection of NMDA, that recovers up to normal levels of expression and total number of m⁺RGCs by 7, 14 days and 15 months. In addition, these results also indicate that m⁺RGCs are resistant to NMMD-induced excitotoxicity. In contrast with the Brn3a⁺RGC population, whose total numbers were reduced to approximately one quarter to one fifth of their normal values, the m⁺RGCs show a complete population that is comparable to that found in their fellow contralateral and in naïve retinas (Figures. 1,3,4, Table 2).

In Vivo SD-OCT measurements

We wanted to examine the effects of the NMDA-induced retinal degeneration on the retinal layers and thus retinas were analysed at 3 and 15 months with SD-OCT to determine the total and inner retinal thickness. Figure 5 shows representative SD-OCT images from both eyes in two representative experimental rats analysed longitudinaly *in vivo* 3 and 15 months after NMDA-injection. The SD-OCT provided measurements of the 31 sections acquired, and we selected three sections located superior, central or inferior for its analysis. Because the measurements of these three sections were comparable within each individual retina and time interval examined, the values from these 3 sections were pooled and used as a value for each retina and time point.

Preprints (www.preprints.org) | NOT PEER-REVIEWED | Posted: 23 May 2019 doi:10.20944/preprints201905.0278.v1

Peer-reviewed version available at Int. J. Mol. Sci. 2019, 20, 3012; doi:10.3390/ijms20123012

Total numbers of Brn3a+RGCs										
	Naïve		3 days		7 days		14 days		15 months	
Retinas	RE	LE	RE	LE	RE	LE	RE	LE	RE	LE
1	80293	82587	72071	46569	74963	24880	71159	16434	89717	14852
2	80399	79044	79209	52957	77604	12227	80940	13785	93939	9538
3	78344	71826	78178		72411	33105	78786	10593	88081	24936
4	74865	77395	79256	19910	66564		73895	39166	81353	21955
5	84031	80247	82406	15648	66086	31097	77579	16132	78436	22369
6			74244	15721	63952	9238	82321		68961	1951
7				62993	71202	20321	87289	15318	83471	5796
8				62344			80773	22261	80699	21478
9				61640			84397	20945		16245
10				12681			80789	12209		24937
11							76135	26641	74808	16594
12									88721	8588
13									75941	1990
14										2754
15									80213	10950
16									81595	5404
17									80424	5584
18									79487	25879
19									79093	25486
20									77667	21966
21									81417	11286
22									83543	25152
23									82032	21587
Mean	78903		77561	38940	70397	21811	79460	19348	81480	15099
± SD	3572		3757	22443	5038	9751	4631	8502	5602	8595
Total RE	**Mean** 78677 **SD** 6260									

Table 1. Total number of Brn3a+RGCs.

Total retinal (TR) thickness (as measured in µm from the inner side of the nerve fibre layer to the outer limit of the outer segment layer) was significantly smaller in the NMDA-injected retinas as compared to their contralateral fellow retinas at 3 (185±4 versus 212±3.2; n=23) and 15 (162±6.1 versus 196±6.1; n=23) months. In fact, the thinning of the TR was mainly due to the thinning of the inner retina (IR) (as measured in µm from the inner side of the nerve fibre layer to the outer limit of the inner nuclear layer). The IR thickness in the left NMDA-injected eyes was significantly smaller than in their fellow retinas at 3 (83±3.7 versus 97±4.2; n=23) and 15 (71±2.8 versus 91±3.4; n=23) months (Figures. 5,6).

The TR thickness of the fellow retinas diminished significantly between 3 (212±3.2; n=23) and 15 (196±6.1; n=23) months, a finding that is in agreement with recent studies in adult albino rats showing a physiological thinning of the TR and IR of approximately 16 and 6 µm, respectively, with age [69]. However, superimposed to the physiological age-related thinning of the retina, in the experimental NMDA-injected retinas there was further significant thinning of the TR (23 µm) and IR (12 µm) between 3 and 15 months (Figures. 5, 6).

Preprints (www.preprints.org) | NOT PEER-REVIEWED | Posted: 23 May 2019 doi:10.20944/preprints201905.0278.v1

Peer-reviewed version available at Int. J. Mol. Sci. 2019, 20, 3012; doi:10.3390/ijms20123012

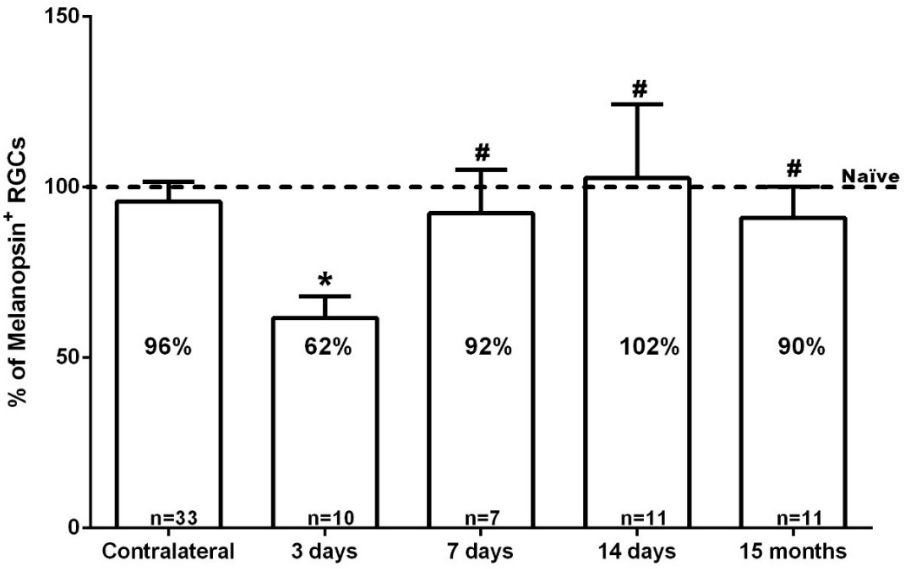

Figure 4. Bar graph showing the percent vs. intact retinas of the total number of m+RGCs ± standard deviation quantified in the contralateral uninjured and experimental retinas analyzed 3, 7, 14 days or 15 months after the intraocular injection of 100 nM NMDA. The number of analyzed retinas is shown at the bottom of each bar. *Significant differences compared to naïve, contralateral retinas and other timepoints (Kruskal-Wallis test, $p<0.001$). # The percent of m+RGCs in the experimental groups analyzed at 7d, 14 days or 15 months did not differ significantly from their contralateral fellow retinas (Mann-Whitney Test, $p>0.05$).

Discussion

Here we have investigated the short- and long-term responses of the populations of Brn3a+ and melanopsin expressing (m+) RGCs after an excitotoxic insult to the retina. Our studies show that following an intraocular injection of 100 nM NMDA, there is a rapid and massive loss of the general population of Brn3a+RGCs; by 3, 14 days or 15 months, the surviving population represents approximately 49%, 28% or 19%, respectively of the original population. When examined with SD-OCT there was an important reduction in the thickness of the total and the inner retina at 3 months that further progressed up to 15 months. Compared to the population of Brn3a+RGCs, m+RGCs show by 3 days a transient downregulation of melanopsin that recovers over the next weeks, and by 14 days or 15 months the numbers of m+RGCs are comparable to their contralateral fellow eyes.

When studying the responses of RGCs to retinal injuries it is important to be able to identify different types of RGCs to understand how these respond to injury [40,70]. Here we use modern techniques developed in the Laboratory to count, image and represent the retinal topography of two RGC populations that can be readily identified with Brn3a and melanopsin [40,71]. Recent studies from this Laboratory have demonstrated that in the adult rat, retinal injuries induce a transient downregulation of melanopsin [28], followed by the expression of melanopsin in injured neurons surviving long periods of time [9,19,72,73]. Of the six main subtypes of ipRGCs M1-M6, immunocytochemistry against melanopsin identifies mainly M1-M3 because they show higher levels of melanopsin expression [32-35,37,38] and thus when interpreting our data, we should take into account that our immunohistochemical methods identify primarily the M1-M3 ipRGC subtypes. In fact, although not analysed in this work, it is conceivable that most of our results refer to the M1 and M2 subtypes which are the most abundant and readily identified with melanopsin antibodies [37,38,74].

Preprints (www.preprints.org) | NOT PEER-REVIEWED | Posted: 23 May 2019 doi:10.20944/preprints201905.0278.v1

Peer-reviewed version available at Int. J. Mol. Sci. 2019, 20, 3012; doi:10.3390/ijms20123012

Total numbers of melanopsin+RGCs										
Retinas	Naive		3 days		7 days		14 days		15 months	
	RE	LE	RE	LE	RE	LE	RE	LE	RE	LE
1	2434	2201	2135	2062	2163	1678	2034	2409		1994
2	2373	2445	1972	1293	2496	1650	2026	2276		2018
3	2366	2103	2294	1187	1962	1860	2055	2149	2154	1997
4	2362	2249	2547	1682	2262	1971	2242	2425	2297	1987
5	2612	2433	1966	1043	2040	2174	2566	2585	2207	1904
6			2183	1448	2471	2662	2363	2145	2016	1857
7				1719	2612	2746	1950	2661	2267	2019
8				1473			2537	2701	2022	2284
9				1850			2267	1955	2156	1961
10				1411			2559	2660	2196	2004
11							2467	2652	2181	2273
Mean	2358		2183	1453	2287	2106	2279	2420	2166	2027
± SD	144		219	371	247	446	235	257	95	133
Total RE	**Mean** 2257 **SD** 229									

Table 2. Total numbers of m+RGCs.

Intravitreal injection of NMDA induces Brn3a+RGC death

The loss of RGCs observed after the injection of NMDA in our studies is comparable to that found by others in mice [56,64] or rat [50,55,75] analysed at survival intervals ranging 3-58 days. We noticed certain inter-animal variability in the total number of surviving Brn3a+RGCs at 3 days after NMDA injection, that was also reported by others [55,64] and could be due to an individual animal susceptibility, or to the fact that RGC loss has not concluded by that time interval. Inter-animal variability following other types of retinal injuries, such as intraorbital optic nerve cut or crush, an insult that results in axotomy of the entire RGC population, have been shown [9,76]. Another possible explanation for the inter-animal variability could be the fact that intravitreal injections may suffer a small reflux of the injected volume rendering the concentration of NMDA not exactly equal for all eyes. We have not investigated shorter survival intervals than 3 days, after NMDA injection, but other studies have suggested that following NMDA injection RGC loss appears as early as 6 hours after injection [77]. It is currently thought that NMDA induced excitotoxicity results in activation of the NMDA receptor and this leads to a massive influx of Ca^{++} that acts as a second messenger to activate pathways that lead to apoptotic neuronal death [78], although the exact signalling pathways involved in NMDA-induced RGC death are not completely understood [58].

Intravitreal injection of NMDA induces a progressive retinal thinning

RGC degeneration results in the loss of neural processes that extend into the inner synaptic layer where they contact cone-bipolar and amacrine cells of different types forming an extensive neuropil that makes up a substantial proportion of the inner synaptic layer's volume. Our results indicate that NMDA-induced retinal excitotoxicity results in a significant decrease of the total (TR) and inner (IR) retinal thickness. This thinning was already apparent in the left NMDA-injected experimental retinas by 3 months when compared to their fellow retinas. The retinal thinning may be explained because over 75% of the Brn3a+RGC population is missing and their dendrites have degenerated thus prompting a thinning of the IPL [75], but also because NMDA-excitotoxiticy results in loss of amacrine cells, as shown with TUNEL and morphometric techniques in adult pigmented mice [82-84] and albino rats [75,85]. The thinning of the TR and IR observed in the fellow retinas between 3 and 15 months is consistent with the physiological thinning of the adult SD rat retina with age [69]. However, superimposed on this physiological thinning, in the experimental retinas there was a progressive thinning of the TR and IR between 3 and 15 months, indicating a continuing retinal

287 degeneration prolonged beyond the time of NMDA injection and the period of Brn3a+RGC loss which
288 concluded by 3 days after the injection. A possible explanation for the progressive thinning of the IR
289 could be the secondary amacrine cell loss that follows RGC death observed after NMDA-induced
290 neurotoxicity. Indeed, approximately 72% of the RGC types in the mice retina are coupled to ACs
291 [86] which may possibly facilitate secondary cell loss of calretinin, calbindin and choline
292 acetyltransferase immunopositive ACs via gap junctions [84].
293

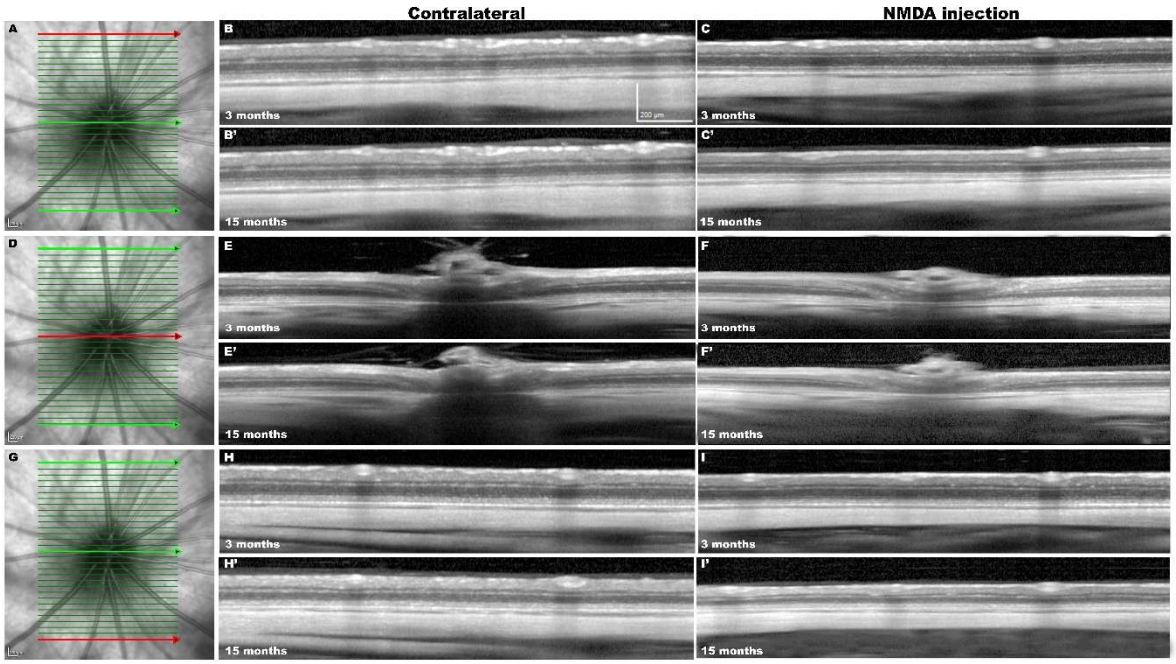

Figure 5. In vivo SD-OCT images from the same contralateral and experimental retinas analyzed 3 and 15 months after NMDA injection. (A, D, G) Representative images of the ocular fundus of the contralateral retina and position of the 31 sections acquired. The superior (A), central (D) or inferior (G) retinal sections are marked in red. (B, C, E, F, H, I) Representative sections acquired (in red) from SD-OCT volume raster scan in contralateral (B, E, H) and NMDA injected (C, F, I) retinas examined longitudinally at 3 (B-I) and at 15 (B'-I') months after NMDA injection

294
295

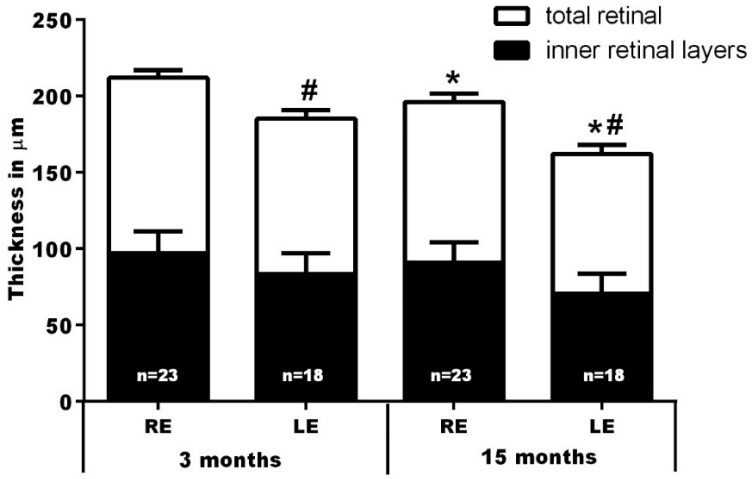

Figure 6. Graph bars showing the reduction of the mean±SD thickness (µm) of the total (from inner side of the nerve fibre layer to outer segment layer) and inner (from the inner side of the nerve fibre layer to outer margin of inner nuclear layer) retina after NMDA intravireal injection into the left eye, measured in the volume scan analyses shown in Figure. 5. *Significant differences compared to the same eyes analyzed at 3 moths (One way Anova Kruskal-Wallis test, $p<0.001$). # Significant differences when compared to their contralateral eyes at the same time interval (Mann-Whitney Rank Sum Test, $p<0.001$). RE, right fellow eye. LE, left eye (NMDA-injected).

m⁺RGCs resilience to retinal disease and injury

In the adult rat m⁺RGCs only represent approximately 2,7% or 2,5% of the total population of RGCS in albino or pigmented, respectively [14,19,69]. Yet, the availability of specific molecular markers for this type of RGCs has made it possible to learn in a very short period of time a great deal about the morphological and functional properties of these neurons, including their idiosyncratic response to different types of inherited or acquired retinal lesions [40]. A number of different laboratories have shown that ipRGCs demonstrate a much better survival against a variety of retinal injuries than the general population of RGCs [87], and this particular resilience has been shown against ocular hypertension in rats [39,88] or mice [89], optic nerve crush or cut in rats [90,91] or mice [35,73,92,93], and transient ischemia of the retina in rats [81]. However, ipRGCs do not appear to be particularly resilient in inherited models of retinal degeneration [94-96], mitochondrial optic neuropathies [97] or degenerative diseases [74] such as Alzheimer [98], Parkinson [99] or Hungtinton [100] disease [74]. A detailed characterization of the RGC responses to NMDA-induced excitotoxicity may shed light into the paradigm of the different responses of different population of RGCs to injury; why some populations die while others survive.

m⁺RGCs are resistant to NMDA-induced retinal excitotoxicity

Our results demonstrate that following a transient downregulation of melanopsin expression, the total number of m⁺RGCs by 14 days or 15 months is comparable to their contralateral fellow eyes, thus indicating an outstanding endurance to NMDA-induced excitotoxicity. Survival of the entire m⁺RGC population by 15 months after NMDA injection is underscored in view of the important inner retinal degeneration and loss of approximately 81% the Brn3a⁺RGC population. The degeneration of RGCs following NMDA-induced excitotoxicity had been explored in adult pigmented mice analyzed at 6 [64] or from 1 to 21 [56] days, respectively. However, these studies showed slight differences in terms of the survival of the m⁺RGC population. DeParis and colleagues [64] found that 6 days after NMDA injection there is a full component of m⁺RGC population surviving in the retina with no downregulation of the expression of melanopsin, while Wang and colleagues [56] reported by 21 days after NMDA injection the loss of approximately one half of the m⁺RGC population. These differences may be explained by the diverse amount of NMDA injected (3µl of 10 mM NMDA versus 1µl of 40 mM NMDA).

The downregulation of melanopsin expression that occurs after retinal injury requires further consideration. Our studies reveal that following NMDA injection there is a transient downregulation of melanopsin that recovers fully by 14 days. A similar transient downregulation of melanopsin has been described in previous studies from this Laboratory in adult rats following optic nerve injury [91], transient elevation of the intraocular pressure [81], the use of retrogradely transported neuronal tracers [101] or acute light-induced retinal degeneration [72]. The differences between our results and those observed by DeParis and colleagues [64] may be a species-specific response of m⁺RGCs, because in parallel studies of m⁺RGCs survival in adult mice following intraorbital optic nerve injury we did not find a transient downregulation of melanopsin [28,73].

Of all the retinal injuries examined so far, m⁺RGCs best afford NMDA-induced excitotoxicity. The reasons for the remarkable resilience of ipRGCs to survive different types of injury-induced retinal degeneration remain an open issue for future studies but several hypotheses have been forwarded to explain m⁺RGCs resilience. One hypothesis proposes that these ipRGCs have large dendrites and axon collaterals within the inner synaptic layer, and thus their intra-retinal connections may be enough to provide trophic support for survival in the absence of brain target derived trophic support [29,87,90,102]. Although it has been postulated that the absence of NMDA receptors in m⁺RGCs could explain its particular resistance to NMDA mediated excitotoxicity, it has been shown that all RGCs express NMDA receptor [103] including m⁺RGCs [63,104] and that the particular resilience of m⁺RGCs is not related to pigmentation, genetic background, the presence of photoreceptors or the activation of the endogenous survival JAK/STAT pathway [64]. Other possible explanations include the activation of PI3K/AKT pathway after optic nerve cut or ocular hypertension [105], but this was not apparent in NMDA-induced excitotoxicity [64]. Melanopsin itself could be thought to have an effect on cell survival, but the fact that many ipRGCs survive with a transient, but lower, expression

of melanopsin makes this unlikely. Another hypothesis explains the resilience on the basis of their neurotransmitter (PACAP) and it is hypothesized that PACAP would act as a neuroprotectant conferring these neurons their particular resistance, since exogenous administration of PACAP protects RGCS against optic nerve transection [106], ocular hypertension [107] or NMDA administration [108]. It could also be possible that different types of RGCs may have different responses to a same insult, thus arguing in favour of a type-specific susceptibility. For example, recent studies using genetic markers to identify different types of RGCs have shown that the type of αRGCs is particularly resistant to NMDA induced neurotoxicity [8] or to optic nerve crush [35,39], in contrast to the very low survival of Junction adhesion molecules B expressing RGCs (J-RGCs) [8]. Moreover, recent studies indicate that among subtypes of ipRGCs there are different susceptibility to specific insults; for instance, in a mouse model of Huntington's disease (HD), M1 were reduced compared to non-M1 ipRGCs which survived to HD progression [109]. Furthermore, in a mouse model of ocular hypertension subtypes of αRGCs were found to have different susceptibility, with OFF-transient αRGCs being more vulnerable than ON- or OFF-sustained αRGCs [22,70]. Overall, the particular resilience of m^+RGCs makes them a suitable candidate to study changes in protein expression after injury to further our knowledge about what makes a neuron survive better than others, and this would in turn result in the design of new neuroprotective strategies for RGCs against noxious stimuli. Thus, future studies are needed to decipher the molecular correlates that provide these neurons with a self-built neuroprotection against various types of injury, including NMDA-induced RGC death.

Material and Methods

Animal handling and experimental groups

Experiments were prepared in 56 adult female SD rats (250g) obtained from the animal house (Murcia University) and treated according to the European Union guidelines for Animal Care and use of scientific purpose (Directive 2010/63/UE). All procedures were approved by the Ethical and Animal Studies Committee of the University of Murcia, Spain. Animals had free access to food and water and kept in a temperature and light controlled room with 12-hr/12-hr light/dark cycles. Animals were anaesthetized with a mixture of xylazine (10mg/kg Rompun; Bayer, Kiel, Germany) and ketamine (60 mg/Kg bw, Ketolar; Pfizer, Alcobendas, Madrid, Spain). 0.5% proparacaine hydrochloride eye drops (Alcon Co., Fort Worth, TX, USA) were used to achieve topical anaesthesia. After the surgical procedures, an ocular ointment was placed over the corneas of both eyes to prevent corneal desiccation (Tobrex®; Alcon-Cusí, S.A., Barcelona, Spain). Animals were divided into experimental and control groups. The experimental group received an intraocular injection of NMDA and was divided into four subgroups that were examined at 3 (n=10), 7 (n=7) or 14 (n=11) days, or 15 months (n=23). Additional naïve rats (n=5) were used as controls. For animal sacrifice an overdose of sodium pentobarbital injected intraperitoneally (Dolethal, Vetoquinol®, Especialidades Veterinarias, S.A., Madrid, Spain).

Intraocular injections of NMDA

Retinal excitotoxicity was induced in the left eye of the experimental animals by intraocular injection of 5 µl of 100nM NMDA N-methyl-D-Aspartate (NMDA) (M3262; Sigma-Aldrich Química S.A., Madrid, Spain) dissolved in 0.1 M phosphate buffer saline (PBS) following standard techniques in our Lab [110-112]. In brief, a small puncture in the sclera approximately 1 mm from the limbus was made with a 30-gauge needle, and then NMDA was injected slowly with a Hamilton syringe whose needle was introduced through the sclerotomy. After injection, the needle was withdrawn slowly and an ointment (Tobrex pomada; Alcon S.A., Barcelona, Spain) was placed over the eyes to prevent corneal dehydration until anaesthesia recovery. The contralateral non-injected eye was used as control, 5 naïve rats (10 eyes) were also used as controls. Preliminary experiments (data not shown) allowed us to try increasing doses of NMDA to find one that would result in consistent RGC death. Previous studies from this Laboratory did not find any effect of the intraocular injection of vehicle alone (0.1 M phosphate buffer saline, PBS) on the survival of the $Brn3a^+$ or $melanopsin^+$ RGC

populations (unpublished observations), and thus, we did not employ additional animals for this purpose.

In vivo measurements of the retinal thickness with SD-OCT

SD-OCT measurements were obtained to analyse changes in the thickness of the retina following NMDA intraocular injection, and the eyes were imaged at 3 and 15 months, as previously described in detail [69,113]. Rats were anaesthetized systemically, and eye drops were placed on both eyes to induce mydriasis (Tropicamida 1%; Alcon-Cusí, S.A.) and to prevent corneal desiccation (artificial tears). Rats were placed in prone position over a platform with their heads upright and turned to the opposite side of the inspected eye. The head position was kept similar for all animals and, and for the following examination the follow up tool of the OCT program was used to compare the same regions. A custom-made permeable contact lens (3.5-mmposterior radius of curvature, 5.0-mm optical zone diameter, 5.0-diopter [D] back vertex power) was placed on the cornea to maintain hydration and thus clarity. Both retinas were imaged using SD-OCT according to the manufacturer instructions (Spectralis; Heidelberg Engineering, Heidelberg, Germany). To adapt for the rat's eye, a commercially available 78-D double aspheric fundus lens (Volk Optical, Inc., Mentor, OH, USA) was mounted in front of the camera unit. Imaging was performed with a software package (EyeExplorer, version 3.2.1.0; Heidelberg Engineering). Retinal thickness was measured using a scanning pattern centred on the optic nerve head; a raster scan of 31 equally spaced horizontal B-scans (3000 μm length). For each section total retinal (TR) (as measured from the inner limiting membrane to the outer limit of the pigmented epithelial layer) and inner retinal (IR) (as measured from the inner limiting membrane to the outer limit of the inner nuclear layer) thickness were measured at distances of 1800 μm from optic disc.

Retinal dissection, immunohistochemistry and image acquisition

At different survival intervals, rats were sacrificed and perfused through the heart, first and briefly with a solution of 0.9% ClNa and then slowly with a 4% paraformaldehyde solution in PBS. The superior pole of the eye was marked with a small suture, and retinas were then dissected and prepared as flattened wholemounts as previously described [114]. Retinas were double-immunodetected following previously described methods for Brn3a and melanopsin to identify surviving RGCS expressing these two markers [14]. Primary antibodies were goat anti-Brn3a (1:750 dilution, C-20 Santa Cruz Biothechology, Heidelberg, Germany) and rabbit anti melanopsin (1:500 dilution, PAI-780, Invitrogen, Thermo Fisher Scientific, Alcobendas, Madrid, Spain). Secondary antibodies were Alexa Fluor conjugated (donkey anti-rabbit Alexa 594, donkey anti-goat Alexa 488) (Molecular Probes Thermo-Fisher, Madrid, Spain). After immunodetection retinas were mounted on subbed slides with the vitreal side up and covered with antifading solution [14].

Photographic reconstructions of flattened whole-mount retinas were obtained under an epifluorescence microscope (Axioscop 2 Plus; Zeiss Mikroscopie, Jena, Germany) equipped with a computer driven motorized stage (ProScan H128 Series; Prior Scientific Instruments, Cambridge, UK) according to previously described methods that are standard in the Lab [73,115]. A total of 154 frames were obtained in the microscope to reconstruct the whole retina. These reconstructions were obtained under both filters to allow identification of Brna3a$^+$RGCs and m$^+$RGCs, respectively. Following standard procedures in the Lab [71,116,117], wholemount reconstructions were further processed to obtain automatically the total number of Brn3a$^+$RGCs and their topographical distribution was represented as isodensity maps. For the m$^+$RGCs, these were quantified manually and dotted on the photomontage with the aid of a graphic editing software Adobe Photoshop CS8.01 (Adobe Systems, Inc., San Jose, CA, USA). Dots were automatically identified, and their topographical distribution represented as neighbour maps following previously described methods [117].

Statistics

Peer-reviewed version available at Int. J. Mol. Sci. 2019, 20, 3012; doi:10.3390/ijms20123012

All data is expressed as means ± standard deviation (SD). Statistical analysis employed the program GraphPad Prism® for windows (Version 5.01; GraphPad Software Inc., La Jolla, CA, EEUU) using non-parametric tests (Kruskal Wallis and Mann Whitney). Differences were considered significant if $p<0.05$.

Conclusions

Intravitreally administered NMDA in adult albino rats: i) induces a massive diffuse loss of Brn3$^+$RGCs already at 3 days that does not progress further; ii) Causes a thinning of the inner retina by 3 months that further progresses up to 15 months; iii) Triggers a transient downregulation of melanopsin expression, that is evident at 3 days and recovers fully by 14 days, and; iv) Does not induce m$^+$RGCs loss.

Back Matter

Supplementary materials

None

Acknowledgements

This study was supported by the Fundación Séneca, Agencia de Ciencia y Tecnología Región de Murcia (19881/GERM/15), and the Spanish Ministry of Economy and Competitiveness, Instituto de Salud Carlos III, Fondo Europeo de Desarrollo Regional "una manera de hacer Europa" (SAF2015-67643-P, PI16/00380, RD16/0008/0026 and RD16/0008/0016).

Author Contributions

BVV, JDP, MVS and NC conceptualized the study. BVV, JDP, FMNN, JAMO, AOM, JMBG, NC, MPVP, and MVS planned and performed all experiments and analysed data. JAMO and AOM performed preliminary experiments to set up the model. JMBG analysed retinas and performed image analysis for RGC counts. BVV, JDP, NC and MVS wrote the paper with input from all authors. MPVP, MVS provided research funds for the study.

Conflicts of Interests

None

References

1. Lucas, R.J.; Peirson, S.N.; Berson, D.M.; Brown, T.M.; Cooper, H.M.; Czeisler, C.A.; Figueiro, M.G.; Gamlin, P.D.; Lockley, S.W.; O'Hagan, J.B., et al. Measuring and using light in the melanopsin age. *Trends in neurosciences* **2014**, *37*, 1-9, doi:10.1016/j.tins.2013.10.004.
2. Smith, C.A.; Chauhan, B.C. Imaging retinal ganglion cells: enabling experimental technology for clinical application. *Progress in retinal and eye research* **2015**, *44*, 1-14, doi:10.1016/j.preteyeres.2014.10.003.
3. Masland, R.H. The neuronal organization of the retina. *Neuron* **2012**, *76*, 266-280, doi:10.1016/j.neuron.2012.10.002.
4. Macosko, E.Z.; Basu, A.; Satija, R.; Nemesh, J.; Shekhar, K.; Goldman, M.; Tirosh, I.; Bialas, A.R.; Kamitaki, N.; Martersteck, E.M., et al. Highly Parallel Genome-wide Expression Profiling of Individual Cells Using Nanoliter Droplets. *Cell* **2015**, *161*, 1202-1214, doi:10.1016/j.cell.2015.05.002.
5. Baden, T.; Berens, P.; Franke, K.; Roman Roson, M.; Bethge, M.; Euler, T. The functional diversity of retinal ganglion cells in the mouse. *Nature* **2016**, *529*, 345-350, doi:10.1038/nature16468.
6. Sanes, J.R.; Masland, R.H. The types of retinal ganglion cells: current status and implications for neuronal classification. *Annual review of neuroscience* **2015**, *38*, 221-246, doi:10.1146/annurev-neuro-071714-034120.
7. Rheaume, B.A.; Jereen, A.; Bolisetty, M.; Sajid, M.S.; Yang, Y.; Renna, K.; Sun, L.; Robson, P.; Trakhtenberg, E.F. Single cell transcriptome profiling of retinal ganglion cells identifies cellular subtypes. *Nature communications* **2018**, *9*, 2759, doi:10.1038/s41467-018-05134-3.
8. Christensen, I.; Lu, B.; Yang, N.; Huang, K.; Wang, P.; Tian, N. The Susceptibility of Retinal Ganglion Cells to Glutamatergic Excitotoxicity Is Type-Specific. *Frontiers in neuroscience* **2019**, *13*, 219, doi:10.3389/fnins.2019.00219.
9. Nadal-Nicolas, F.M.; Salinas-Navarro, M.; Vidal-Sanz, M.; Agudo-Barriuso, M. Two methods to trace retinal ganglion cells with fluorogold: from the intact optic nerve or by stereotactic injection into the optic tract. *Experimental eye research* **2015**, *131*, 12-19, doi:10.1016/j.exer.2014.12.005.
10. Thanos, S.; Vidal-Sanz, M.; Aguayo, A.J. The use of rhodamine-B-isothiocyanate (RITC) as an anterograde and retrograde tracer in the adult rat visual system. *Brain research* **1987**, *406*, 317-321.
11. Vidal-Sanz, M.; Bray, G.M.; Villegas-Perez, M.P.; Thanos, S.; Aguayo, A.J. Axonal regeneration and synapse formation in the superior colliculus by retinal ganglion cells in the adult rat. *The Journal of neuroscience : the official journal of the Society for Neuroscience* **1987**, *7*, 2894-2909.
12. Barnstable, C.J.; Drager, U.C. Thy-1 antigen: a ganglion cell specific marker in rodent retina. *Neuroscience* **1984**, *11*, 847-855.
13. Nadal-Nicolas, F.M.; Jimenez-Lopez, M.; Salinas-Navarro, M.; Sobrado-Calvo, P.; Alburquerque-Bejar, J.J.; Vidal-Sanz, M.; Agudo-Barriuso, M. Whole number, distribution and co-expression of brn3 transcription factors in retinal ganglion cells of adult albino and pigmented rats. *PloS one* **2012**, *7*, e49830, doi:10.1371/journal.pone.0049830.
14. Nadal-Nicolas, F.M.; Salinas-Navarro, M.; Jimenez-Lopez, M.; Sobrado-Calvo, P.; Villegas-Perez, M.P.; Vidal-Sanz, M.; Agudo-Barriuso, M. Displaced retinal ganglion cells in albino and pigmented rats. *Frontiers in neuroanatomy* **2014**, *8*, 99, doi:10.3389/fnana.2014.00099.
15. Rodriguez, A.R.; de Sevilla Muller, L.P.; Brecha, N.C. The RNA binding protein RBPMS is a selective marker of ganglion cells in the mammalian retina. *The Journal of comparative neurology* **2014**, *522*, 1411-1443, doi:10.1002/cne.23521.

16. Jiang, S.M.; Zeng, L.P.; Zeng, J.H.; Tang, L.; Chen, X.M.; Wei, X. beta-III-Tubulin: a reliable marker for retinal ganglion cell labeling in experimental models of glaucoma. *International journal of ophthalmology* **2015**, *8*, 643-652, doi:10.3980/j.issn.2222-3959.2015.04.01.
17. Dijk, F.; Bergen, A.A.; Kamphuis, W. GAP-43 expression is upregulated in retinal ganglion cells after ischemia/reperfusion-induced damage. *Experimental eye research* **2007**, *84*, 858-867, doi:10.1016/j.exer.2007.01.006.
18. McKerracher, L.; Vallee, R.B.; Aguayo, A.J. Microtubule-associated protein 1A (MAP 1A) is a ganglion cell marker in adult rat retina. *Visual neuroscience* **1989**, *2*, 349-356.
19. Galindo-Romero, C.; Jimenez-Lopez, M.; Garcia-Ayuso, D.; Salinas-Navarro, M.; Nadal-Nicolas, F.M.; Agudo-Barriuso, M.; Villegas-Perez, M.P.; Aviles-Trigueros, M.; Vidal-Sanz, M. Number and spatial distribution of intrinsically photosensitive retinal ganglion cells in the adult albino rat. *Experimental eye research* **2013**, *108*, 84-93, doi:10.1016/j.exer.2012.12.010.
20. Kim, I.J.; Zhang, Y.; Yamagata, M.; Meister, M.; Sanes, J.R. Molecular identification of a retinal cell type that responds to upward motion. *Nature* **2008**, *452*, 478-482, doi:10.1038/nature06739.
21. Agostinone, J.; Di Polo, A. Retinal ganglion cell dendrite pathology and synapse loss: Implications for glaucoma. *Progress in brain research* **2015**, *220*, 199-216, doi:10.1016/bs.pbr.2015.04.012.
22. Ou, Y.; Jo, R.E.; Ullian, E.M.; Wong, R.O.; Della Santina, L. Selective Vulnerability of Specific Retinal Ganglion Cell Types and Synapses after Transient Ocular Hypertension. *The Journal of neuroscience : the official journal of the Society for Neuroscience* **2016**, *36*, 9240-9252, doi:10.1523/JNEUROSCI.0940-16.2016.
23. Chidlow, G.; Casson, R.; Sobrado-Calvo, P.; Vidal-Sanz, M.; Osborne, N.N. Measurement of retinal injury in the rat after optic nerve transection: an RT-PCR study. *Molecular vision* **2005**, *11*, 387-396.
24. Lonngren, U.; Napankangas, U.; Lafuente, M.; Mayor, S.; Lindqvist, N.; Vidal-Sanz, M.; Hallbook, F. The growth factor response in ischemic rat retina and superior colliculus after brimonidine pre-treatment. *Brain research bulletin* **2006**, *71*, 208-218, doi:10.1016/j.brainresbull.2006.09.005.
25. Agudo, M.; Perez-Marin, M.C.; Lonngren, U.; Sobrado, P.; Conesa, A.; Canovas, I.; Salinas-Navarro, M.; Miralles-Imperial, J.; Hallbook, F.; Vidal-Sanz, M. Time course profiling of the retinal transcriptome after optic nerve transection and optic nerve crush. *Molecular vision* **2008**, *14*, 1050-1063.
26. Agudo, M.; Perez-Marin, M.C.; Sobrado-Calvo, P.; Lonngren, U.; Salinas-Navarro, M.; Canovas, I.; Nadal-Nicolas, F.M.; Miralles-Imperial, J.; Hallbook, F.; Vidal-Sanz, M. Immediate upregulation of proteins belonging to different branches of the apoptotic cascade in the retina after optic nerve transection and optic nerve crush. *Investigative ophthalmology & visual science* **2009**, *50*, 424-431, doi:10.1167/iovs.08-2404.
27. Agudo-Barriuso, M.; Lahoz, A.; Nadal-Nicolas, F.M.; Sobrado-Calvo, P.; Piquer-Gil, M.; Diaz-Llopis, M.; Vidal-Sanz, M.; Mullor, J.L. Metabolomic changes in the rat retina after optic nerve crush. *Investigative ophthalmology & visual science* **2013**, *54*, 4249-4259, doi:10.1167/iovs.12-11451.
28. Agudo-Barriuso, M.; Nadal-Nicolas, F.M.; Madeira, M.H.; Rovere, G.; Vidal-Villegas, B.; Vidal-Sanz, M. Melanopsin expression is an indicator of the well-being of melanopsin-expressing retinal ganglion cells but not of their viability. *Neural regeneration research* **2016**, *11*, 1243-1244, doi:10.4103/1673-5374.189182.
29. Vugler, A.; Semo, M.; Ortin-Martinez, A.; Rojanasakul, A.; Nommiste, B.; Valiente-Soriano, F.J.; Garcia-Ayuso, D.; Coffey, P.; Vidal-Sanz, M.; Gias, C. A role for the outer retina in

development of the intrinsic pupillary light reflex in mice. *Neuroscience* **2015**, *286*, 60-78, doi:10.1016/j.neuroscience.2014.11.044.

30. Hannibal, J.; Christiansen, A.T.; Heegaard, S.; Fahrenkrug, J.; Kiilgaard, J.F. Melanopsin expressing human retinal ganglion cells: Subtypes, distribution, and intraretinal connectivity. *The Journal of comparative neurology* **2017**, *525*, 1934-1961, doi:10.1002/cne.24181.
31. Berson, D.M.; Castrucci, A.M.; Provencio, I. Morphology and mosaics of melanopsin-expressing retinal ganglion cell types in mice. *The Journal of comparative neurology* **2010**, *518*, 2405-2422, doi:10.1002/cne.22381.
32. Quattrochi, L.E.; Stabio, M.E.; Kim, I.; Ilardi, M.C.; Michelle Fogerson, P.; Leyrer, M.L.; Berson, D.M. The M6 cell: A small-field bistratified photosensitive retinal ganglion cell. *The Journal of comparative neurology* **2019**, *527*, 297-311, doi:10.1002/cne.24556.
33. Sonoda, T.; Lee, S.K.; Birnbaumer, L.; Schmidt, T.M. Melanopsin Phototransduction Is Repurposed by ipRGC Subtypes to Shape the Function of Distinct Visual Circuits. *Neuron* **2018**, *99*, 754-767 e754, doi:10.1016/j.neuron.2018.06.032.
34. Estevez, M.E.; Fogerson, P.M.; Ilardi, M.C.; Borghuis, B.G.; Chan, E.; Weng, S.; Auferkorte, O.N.; Demb, J.B.; Berson, D.M. Form and function of the M4 cell, an intrinsically photosensitive retinal ganglion cell type contributing to geniculocortical vision. *The Journal of neuroscience : the official journal of the Society for Neuroscience* **2012**, *32*, 13608-13620, doi:10.1523/JNEUROSCI.1422-12.2012.
35. Duan, X.; Qiao, M.; Bei, F.; Kim, I.J.; He, Z.; Sanes, J.R. Subtype-specific regeneration of retinal ganglion cells following axotomy: effects of osteopontin and mTOR signaling. *Neuron* **2015**, *85*, 1244-1256, doi:10.1016/j.neuron.2015.02.017.
36. Berry, M.; Ahmed, Z.; Logan, A. Return of function after CNS axon regeneration: Lessons from injury-responsive intrinsically photosensitive and alpha retinal ganglion cells. *Progress in retinal and eye research* **2018**, 10.1016/j.preteyeres.2018.11.006, doi:10.1016/j.preteyeres.2018.11.006.
37. Schmidt, T.M.; Chen, S.K.; Hattar, S. Intrinsically photosensitive retinal ganglion cells: many subtypes, diverse functions. *Trends in neurosciences* **2011**, *34*, 572-580, doi:10.1016/j.tins.2011.07.001.
38. Schmidt, T.M.; Do, M.T.; Dacey, D.; Lucas, R.; Hattar, S.; Matynia, A. Melanopsin-positive intrinsically photosensitive retinal ganglion cells: from form to function. *The Journal of neuroscience : the official journal of the Society for Neuroscience* **2011**, *31*, 16094-16101, doi:10.1523/JNEUROSCI.4132-11.2011.
39. Li, S.; Yang, C.; Zhang, L.; Gao, X.; Wang, X.; Liu, W.; Wang, Y.; Jiang, S.; Wong, Y.H.; Zhang, Y., et al. Promoting axon regeneration in the adult CNS by modulation of the melanopsin/GPCR signaling. *Proceedings of the National Academy of Sciences of the United States of America* **2016**, *113*, 1937-1942, doi:10.1073/pnas.1523645113.
40. Vidal-Sanz, M.; Nadal-Nicolas, F.M.; Valiente-Soriano, F.J.; Agudo-Barriuso, M.; Villegas-Perez, M.P. Identifying specific RGC types may shed light on their idiosyncratic responses to neuroprotection. *Neural regeneration research* **2015**, *10*, 1228-1230, doi:10.4103/1673-5374.162751.
41. Lucas, D.R.; Newhouse, J.P. The toxic effect of sodium L-glutamate on the inner layers of the retina. *A.M.A. archives of ophthalmology* **1957**, *58*, 193-201.
42. Choi, D.W. Glutamate neurotoxicity and diseases of the nervous system. *Neuron* **1988**, *1*, 623-634.
43. Dreyer, E.B.; Zurakowski, D.; Schumer, R.A.; Podos, S.M.; Lipton, S.A. Elevated glutamate levels in the vitreous body of humans and monkeys with glaucoma. *Arch Ophthalmol* **1996**, *114*, 299-305.

44. Izzotti, A.; Bagnis, A.; Sacca, S.C. The role of oxidative stress in glaucoma. *Mutation research* **2006**, *612*, 105-114, doi:10.1016/j.mrrev.2005.11.001.
45. Tezel, G. Immune regulation toward immunomodulation for neuroprotection in glaucoma. *Current opinion in pharmacology* **2013**, *13*, 23-31, doi:10.1016/j.coph.2012.09.013.
46. Vorwerk, C.K.; Kreutz, M.R.; Bockers, T.M.; Brosz, M.; Dreyer, E.B.; Sabel, B.A. Susceptibility of retinal ganglion cells to excitotoxicity depends on soma size and retinal eccentricity. *Current eye research* **1999**, *19*, 59-65.
47. Vorwerk, C.K.; Zurakowski, D.; McDermott, L.M.; Mawrin, C.; Dreyer, E.B. Effects of axonal injury on ganglion cell survival and glutamate homeostasis. *Brain research bulletin* **2004**, *62*, 485-490, doi:10.1016/S0361-9230(03)00075-3.
48. Lam, T.T.; Siew, E.; Chu, R.; Tso, M.O. Ameliorative effect of MK-801 on retinal ischemia. *Journal of ocular pharmacology and therapeutics : the official journal of the Association for Ocular Pharmacology and Therapeutics* **1997**, *13*, 129-137, doi:10.1089/jop.1997.13.129.
49. Schuettauf, F.; Naskar, R.; Vorwerk, C.K.; Zurakowski, D.; Dreyer, E.B. Ganglion cell loss after optic nerve crush mediated through AMPA-kainate and NMDA receptors. *Investigative ophthalmology & visual science* **2000**, *41*, 4313-4316.
50. Kermer, P.; Klocker, N.; Bahr, M. Modulation of metabotropic glutamate receptors fails to prevent the loss of adult rat retinal ganglion cells following axotomy or N-methyl-D-aspartate lesion in vivo. *Neuroscience letters* **2001**, *315*, 117-120.
51. Almasieh, M.; Wilson, A.M.; Morquette, B.; Cueva Vargas, J.L.; Di Polo, A. The molecular basis of retinal ganglion cell death in glaucoma. *Progress in retinal and eye research* **2012**, *31*, 152-181, doi:10.1016/j.preteyeres.2011.11.002.
52. Manev, H.; Favaron, M.; Guidotti, A.; Costa, E. Delayed increase of Ca2+ influx elicited by glutamate: role in neuronal death. *Molecular pharmacology* **1989**, *36*, 106-112.
53. Stavrovskaya, I.G.; Kristal, B.S. The powerhouse takes control of the cell: is the mitochondrial permeability transition a viable therapeutic target against neuronal dysfunction and death? *Free radical biology & medicine* **2005**, *38*, 687-697, doi:10.1016/j.freeradbiomed.2004.11.032.
54. Hardingham, G.E.; Fukunaga, Y.; Bading, H. Extrasynaptic NMDARs oppose synaptic NMDARs by triggering CREB shut-off and cell death pathways. *Nature neuroscience* **2002**, *5*, 405-414, doi:10.1038/nn835.
55. Gomez-Vicente, V.; Lax, P.; Fernandez-Sanchez, L.; Rondon, N.; Esquiva, G.; Germain, F.; de la Villa, P.; Cuenca, N. Neuroprotective Effect of Tauroursodeoxycholic Acid on N-Methyl-D-Aspartate-Induced Retinal Ganglion Cell Degeneration. *PloS one* **2015**, *10*, e0137826, doi:10.1371/journal.pone.0137826.
56. Wang, S.; Gu, D.; Zhang, P.; Chen, J.; Li, Y.; Xiao, H.; Zhou, G. Melanopsin-expressing retinal ganglion cells are relatively resistant to excitotoxicity induced by N-methyl-d-aspartate. *Neuroscience letters* **2018**, *662*, 368-373, doi:10.1016/j.neulet.2017.10.055.
57. Pichavaram, P.; Palani, C.D.; Patel, C.; Xu, Z.; Shosha, E.; Fouda, A.Y.; Caldwell, R.B.; Narayanan, S.P. Targeting Polyamine Oxidase to Prevent Excitotoxicity-Induced Retinal Neurodegeneration. *Frontiers in neuroscience* **2018**, *12*, 956, doi:10.3389/fnins.2018.00956.
58. Fahrenthold, B.K.; Fernandes, K.A.; Libby, R.T. Assessment of intrinsic and extrinsic signaling pathway in excitotoxic retinal ganglion cell death. *Scientific reports* **2018**, *8*, 4641, doi:10.1038/s41598-018-22848-y.
59. Kobayashi, M.; Hirooka, K.; Ono, A.; Nakano, Y.; Nishiyama, A.; Tsujikawa, A. The Relationship Between the Renin-Angiotensin-Aldosterone System and NMDA Receptor-Mediated Signal and the Prevention of Retinal Ganglion Cell Death. *Investigative ophthalmology & visual science* **2017**, *58*, 1397-1403, doi:10.1167/iovs.16-21001.

60. Manabe, S.; Gu, Z.; Lipton, S.A. Activation of matrix metalloproteinase-9 via neuronal nitric oxide synthase contributes to NMDA-induced retinal ganglion cell death. *Investigative ophthalmology & visual science* **2005**, *46*, 4747-4753, doi:10.1167/iovs.05-0128.
61. Lambuk, L.; Iezhitsa, I.; Agarwal, R.; Bakar, N.S.; Agarwal, P.; Ismail, N.M. Antiapoptotic effect of taurine against NMDA-induced retinal excitotoxicity in rats. *Neurotoxicology* **2019**, *70*, 62-71, doi:10.1016/j.neuro.2018.10.009.
62. Tsoka, P.; Barbisan, P.R.; Kataoka, K.; Chen, X.N.; Tian, B.; Bouzika, P.; Miller, J.W.; Paschalis, E.I.; Vavvas, D.G. NLRP3 inflammasome in NMDA-induced retinal excitotoxicity. *Experimental eye research* **2019**, *181*, 136-144, doi:10.1016/j.exer.2019.01.018.
63. Ito, A.; Tsuda, S.; Kunikata, H.; Toshifumi, A.; Sato, K.; Nakazawa, T. Assessing retinal ganglion cell death and neuroprotective agents using real time imaging. *Brain research* **2019**, *1714*, 65-72, doi:10.1016/j.brainres.2019.02.008.
64. DeParis, S.; Caprara, C.; Grimm, C. Intrinsically photosensitive retinal ganglion cells are resistant to N-methyl-D-aspartic acid excitotoxicity. *Molecular vision* **2012**, *18*, 2814-2827.
65. Vidal-Villegas, B., Miralles de Imperial-Ollero, J.A., Nadal-Nicolás, F.M., Ortín-Martínez, A., Bernal-Garro, J.M., Vidal-Sanz, M., Villegas-Pérez, M.P. Effectss of intravitreal injections of N-Methyl-D-Aspartate on melanopsin and non-melanopsin containing retinal ganglion cells in the adult rat. *Ophtalmic Res*. **2017**, 57,25.
66. Salinas-Navarro, M.; Mayor-Torroglosa, S.; Jimenez-Lopez, M.; Aviles-Trigueros, M.; Holmes, T.M.; Lund, R.D.; Villegas-Perez, M.P.; Vidal-Sanz, M. A computerized analysis of the entire retinal ganglion cell population and its spatial distribution in adult rats. *Vision research* **2009**, *49*, 115-126, doi:10.1016/j.visres.2008.09.029.
67. Nadal-Nicolas, F.M.; Jimenez-Lopez, M.; Sobrado-Calvo, P.; Nieto-Lopez, L.; Canovas-Martinez, I.; Salinas-Navarro, M.; Vidal-Sanz, M.; Agudo, M. Brn3a as a marker of retinal ganglion cells: qualitative and quantitative time course studies in naive and optic nerve-injured retinas. *Investigative ophthalmology & visual science* **2009**, *50*, 3860-3868, doi:10.1167/iovs.08-3267.
68. Ortin-Martinez, A.; Jimenez-Lopez, M.; Nadal-Nicolas, F.M.; Salinas-Navarro, M.; Alarcon-Martinez, L.; Sauve, Y.; Villegas-Perez, M.P.; Vidal-Sanz, M.; Agudo-Barriuso, M. Automated quantification and topographical distribution of the whole population of S- and L-cones in adult albino and pigmented rats. *Investigative ophthalmology & visual science* **2010**, *51*, 3171-3183, doi:10.1167/iovs.09-4861.
69. Nadal-Nicolas, F.M.; Vidal-Sanz, M.; Agudo-Barriuso, M. The aging rat retina: from function to anatomy. *Neurobiology of aging* **2018**, *61*, 146-168, doi:10.1016/j.neurobiolaging.2017.09.021.
70. Della Santina, L.; Ou, Y. Who's lost first? Susceptibility of retinal ganglion cell types in experimental glaucoma. *Experimental eye research* **2017**, *158*, 43-50, doi:10.1016/j.exer.2016.06.006.
71. Vidal-Sanz, M.; Galindo-Romero, C.; Valiente-Soriano, F.J.; Nadal-Nicolas, F.M.; Ortin-Martinez, A.; Rovere, G.; Salinas-Navarro, M.; Lucas-Ruiz, F.; Sanchez-Migallon, M.C.; Sobrado-Calvo, P., et al. Shared and Differential Retinal Responses against Optic Nerve Injury and Ocular Hypertension. *Frontiers in neuroscience* **2017**, *11*, 235, doi:10.3389/fnins.2017.00235.
72. Garcia-Ayuso, D.; Galindo-Romero, C.; Di Pierdomenico, J.; Vidal-Sanz, M.; Agudo-Barriuso, M.; Villegas Perez, M.P. Light-induced retinal degeneration causes a transient downregulation of melanopsin in the rat retina. *Experimental eye research* **2017**, *161*, 10-16, doi:10.1016/j.exer.2017.05.010.
73. Sanchez-Migallon, M.C.; Valiente-Soriano, F.J.; Nadal-Nicolas, F.M.; Di Pierdomenico, J.; Vidal-Sanz, M.; Agudo-Barriuso, M. Survival of melanopsin expressing retinal ganglion

729 cells long term after optic nerve trauma in mice. *Experimental eye research* **2018**, *174*, 93-97,
730 doi:10.1016/j.exer.2018.05.029.
731 74. Lax, P., Ortuño-Lizarán, I., Maneu, V., Vidal-Sanzm M., Cuenca, N. Melanopsin-containing
732 ganglion cells in the healthy and disease retina. *International Journal of Molecular Sciences*
733 **2019** (*Submitted*).
734 75. Huang, W.; Hu, F.; Wang, M.; Gao, F.; Xu, P.; Xing, C.; Sun, X.; Zhang, S.; Wu, J.
735 Comparative analysis of retinal ganglion cell damage in three glaucomatous rat models.
736 *Experimental eye research* **2018**, *172*, 112-122, doi:10.1016/j.exer.2018.03.019.
737 76. Villegas-Perez, M.P.; Vidal-Sanz, M.; Rasminsky, M.; Bray, G.M.; Aguayo, A.J. Rapid and
738 protracted phases of retinal ganglion cell loss follow axotomy in the optic nerve of adult
739 rats. *Journal of neurobiology* **1993**, *24*, 23-36, doi:10.1002/neu.480240103.
740 77. Endo, K.; Nakamachi, T.; Seki, T.; Kagami, N.; Wada, Y.; Nakamura, K.; Kishimoto, K.;
741 Hori, M.; Tsuchikawa, D.; Shinntani, N., et al. Neuroprotective effect of PACAP against
742 NMDA-induced retinal damage in the mouse. *Journal of molecular neuroscience : MN* **2011**,
743 *43*, 22-29, doi:10.1007/s12031-010-9434-x.
744 78. Lebrun-Julien, F.; Duplan, L.; Pernet, V.; Osswald, I.; Sapieha, P.; Bourgeois, P.; Dickson, K.;
745 Bowie, D.; Barker, P.A.; Di Polo, A. Excitotoxic death of retinal neurons in vivo occurs via a
746 non-cell-autonomous mechanism. *The Journal of neuroscience : the official journal of the Society*
747 *for Neuroscience* **2009**, *29*, 5536-5545, doi:10.1523/JNEUROSCI.0831-09.2009.
748 79. Salinas-Navarro, M.; Alarcon-Martinez, L.; Valiente-Soriano, F.J.; Jimenez-Lopez, M.;
749 Mayor-Torroglosa, S.; Aviles-Trigueros, M.; Villegas-Perez, M.P.; Vidal-Sanz, M. Ocular
750 hypertension impairs optic nerve axonal transport leading to progressive retinal ganglion
751 cell degeneration. *Experimental eye research* **2010**, *90*, 168-183, doi:10.1016/j.exer.2009.10.003.
752 80. Cuenca, N.; Pinilla, I.; Fernandez-Sanchez, L.; Salinas-Navarro, M.; Alarcon-Martinez, L.;
753 Aviles-Trigueros, M.; de la Villa, P.; Miralles de Imperial, J.; Villegas-Perez, M.P.; Vidal-
754 Sanz, M. Changes in the inner and outer retinal layers after acute increase of the intraocular
755 pressure in adult albino Swiss mice. *Experimental eye research* **2010**, *91*, 273-285,
756 doi:10.1016/j.exer.2010.05.020.
757 81. Rovere, G.; Nadal-Nicolas, F.M.; Wang, J.; Bernal-Garro, J.M.; Garcia-Carrillo, N.; Villegas-
758 Perez, M.P.; Agudo-Barriuso, M.; Vidal-Sanz, M. Melanopsin-Containing or Non-
759 Melanopsin-Containing Retinal Ganglion Cells Response to Acute Ocular Hypertension
760 With or Without Brain-Derived Neurotrophic Factor Neuroprotection. *Investigative*
761 *ophthalmology & visual science* **2016**, *57*, 6652-6661, doi:10.1167/iovs.16-20146.
762 82. Lam, T.T.; Abler, A.S.; Kwong, J.M.; Tso, M.O. N-methyl-D-aspartate (NMDA)--induced
763 apoptosis in rat retina. *Investigative ophthalmology & visual science* **1999**, *40*, 2391-2397.
764 83. Li, Y.; Schlamp, C.L.; Nickells, R.W. Experimental induction of retinal ganglion cell death in
765 adult mice. *Investigative ophthalmology & visual science* **1999**, *40*, 1004-1008.
766 84. Akopian, A.; Atlasz, T.; Pan, F.; Wong, S.; Zhang, Y.; Volgyi, B.; Paul, D.L.; Bloomfield, S.A.
767 Gap junction-mediated death of retinal neurons is connexin and insult specific: a potential
768 target for neuroprotection. *The Journal of neuroscience : the official journal of the Society for*
769 *Neuroscience* **2014**, *34*, 10582-10591, doi:10.1523/JNEUROSCI.1912-14.2014.
770 85. Siliprandi, R.; Canella, R.; Carmignoto, G.; Schiavo, N.; Zanellato, A.; Zanoni, R.; Vantini, G.
771 N-methyl-D-aspartate-induced neurotoxicity in the adult rat retina. *Visual neuroscience* **1992**,
772 *8*, 567-573.
773 86. Volgyi, B.; Chheda, S.; Bloomfield, S.A. Tracer coupling patterns of the ganglion cell
774 subtypes in the mouse retina. *The Journal of comparative neurology* **2009**, *512*, 664-687,
775 doi:10.1002/cne.21912.

87. Cui, Q.; Ren, C.; Sollars, P.J.; Pickard, G.E.; So, K.F. The injury resistant ability of melanopsin-expressing intrinsically photosensitive retinal ganglion cells. *Neuroscience* **2015**, *284*, 845-853, doi:10.1016/j.neuroscience.2014.11.002.
88. Valiente-Soriano, F.J.; Nadal-Nicolas, F.M.; Salinas-Navarro, M.; Jimenez-Lopez, M.; Bernal-Garro, J.M.; Villegas-Perez, M.P.; Agudo-Barriuso, M.; Vidal-Sanz, M. BDNF Rescues RGCs But Not Intrinsically Photosensitive RGCs in Ocular Hypertensive Albino Rat Retinas. *Investigative ophthalmology & visual science* **2015**, *56*, 1924-1936, doi:10.1167/iovs.15-16454.
89. Jakobs, T.C.; Ben, Y.; Masland, R.H. Expression of mRNA for glutamate receptor subunits distinguishes the major classes of retinal neurons, but is less specific for individual cell types. *Molecular vision* **2007**, *13*, 933-948.
90. Perez de Sevilla Muller, L.; Sargoy, A.; Rodriguez, A.R.; Brecha, N.C. Melanopsin ganglion cells are the most resistant retinal ganglion cell type to axonal injury in the rat retina. *PloS one* **2014**, *9*, e93274, doi:10.1371/journal.pone.0093274.
91. Nadal-Nicolas, F.M.; Sobrado-Calvo, P.; Jimenez-Lopez, M.; Vidal-Sanz, M.; Agudo-Barriuso, M. Long-Term Effect of Optic Nerve Axotomy on the Retinal Ganglion Cell Layer. *Investigative ophthalmology & visual science* **2015**, *56*, 6095-6112, doi:10.1167/iovs.15-17195.
92. Robinson, G.A.; Madison, R.D. Axotomized mouse retinal ganglion cells containing melanopsin show enhanced survival, but not enhanced axon regrowth into a peripheral nerve graft. *Vision research* **2004**, *44*, 2667-2674, doi:10.1016/j.visres.2004.06.010.
93. Daniel, S.; Clark, A.F.; McDowell, C.M. Subtype-specific response of retinal ganglion cells to optic nerve crush. *Cell death discovery* **2018**, *4*, 7, doi:10.1038/s41420-018-0069-y.
94. Vugler, A.A.; Semo, M.; Joseph, A.; Jeffery, G. Survival and remodeling of melanopsin cells during retinal dystrophy. *Visual neuroscience* **2008**, *25*, 125-138, doi:10.1017/S0952523808080309.
95. Esquiva, G.; Lax, P.; Cuenca, N. Impairment of intrinsically photosensitive retinal ganglion cells associated with late stages of retinal degeneration. *Investigative ophthalmology & visual science* **2013**, *54*, 4605-4618, doi:10.1167/iovs.13-12120.
96. Garcia-Ayuso, D.; Di Pierdomenico, J.; Esquiva, G.; Nadal-Nicolas, F.M.; Pinilla, I.; Cuenca, N.; Vidal-Sanz, M.; Agudo-Barriuso, M.; Villegas-Perez, M.P. Inherited Photoreceptor Degeneration Causes the Death of Melanopsin-Positive Retinal Ganglion Cells and Increases Their Coexpression of Brn3a. *Investigative ophthalmology & visual science* **2015**, *56*, 4592-4604, doi:10.1167/iovs.15-16808.
97. La Morgia, C.; Ross-Cisneros, F.N.; Sadun, A.A.; Hannibal, J.; Munarini, A.; Mantovani, V.; Barboni, P.; Cantalupo, G.; Tozer, K.R.; Sancisi, E., et al. Melanopsin retinal ganglion cells are resistant to neurodegeneration in mitochondrial optic neuropathies. *Brain : a journal of neurology* **2010**, *133*, 2426-2438, doi:10.1093/brain/awq155.
98. Georg, B.; Ghelli, A.; Giordano, C.; Ross-Cisneros, F.N.; Sadun, A.A.; Carelli, V.; Hannibal, J.; La Morgia, C. Melanopsin-expressing retinal ganglion cells are resistant to cell injury, but not always. *Mitochondrion* **2017**, *36*, 77-84, doi:10.1016/j.mito.2017.04.003.
99. Lax, P.; Esquiva, G.; Esteve-Rudd, J.; Otalora, B.B.; Madrid, J.A.; Cuenca, N. Circadian dysfunction in a rotenone-induced parkinsonian rodent model. *Chronobiology international* **2012**, *29*, 147-156, doi:10.3109/07420528.2011.649870.
100. Wulff, K.; Gatti, S.; Wettstein, J.G.; Foster, R.G. Sleep and circadian rhythm disruption in psychiatric and neurodegenerative disease. *Nature reviews. Neuroscience* **2010**, *11*, 589-599, doi:10.1038/nrn2868.
101. Nadal-Nicolas, F.M.; Madeira, M.H.; Salinas-Navarro, M.; Jimenez-Lopez, M.; Galindo-Romero, C.; Ortin-Martinez, A.; Santiago, A.R.; Vidal-Sanz, M.; Agudo-Barriuso, M. Transient Downregulation of Melanopsin Expression After Retrograde Tracing or Optic

Nerve Injury in Adult Rats. Investigative ophthalmology & visual science 2015, 56, 4309-4323, doi:10.1167/iovs.15-16963.

102. Semo, M.; Gias, C.; Ahmado, A.; Vugler, A. A role for the ciliary marginal zone in the melanopsin-dependent intrinsic pupillary light reflex. Experimental eye research 2014, 119, 8-18, doi:10.1016/j.exer.2013.11.013.
103. Zhang, J.; Diamond, J.S. Subunit- and pathway-specific localization of NMDA receptors and scaffolding proteins at ganglion cell synapses in rat retina. The Journal of neuroscience : the official journal of the Society for Neuroscience 2009, 29, 4274-4286, doi:10.1523/JNEUROSCI.5602-08.2009.
104. Jakobs, T.C.; Libby, R.T.; Ben, Y.; John, S.W.; Masland, R.H. Retinal ganglion cell degeneration is topological but not cell type specific in DBA/2J mice. The Journal of cell biology 2005, 171, 313-325, doi:10.1083/jcb.200506099.
105. Li, S.Y.; Yau, S.Y.; Chen, B.Y.; Tay, D.K.; Lee, V.W.; Pu, M.L.; Chan, H.H.; So, K.F. Enhanced survival of melanopsin-expressing retinal ganglion cells after injury is associated with the PI3 K/Akt pathway. Cellular and molecular neurobiology 2008, 28, 1095-1107, doi:10.1007/s10571-008-9286-x.
106. Seki, T.; Nakatani, M.; Taki, C.; Shinohara, Y.; Ozawa, M.; Nishimura, S.; Ito, H.; Shioda, S. Neuroprotective effect of PACAP against kainic acid-induced neurotoxicity in rat retina. Annals of the New York Academy of Sciences 2006, 1070, 531-534, doi:10.1196/annals.1317.074.
107. Nakatani, M.; Seki, T.; Shinohara, Y.; Taki, C.; Nishimura, S.; Takaki, A.; Shioda, S. Pituitary adenylate cyclase-activating peptide (PACAP) stimulates production of interleukin-6 in rat Muller cells. Peptides 2006, 27, 1871-1876, doi:10.1016/j.peptides.2005.12.011.
108. Belenky, M.A.; Smeraski, C.A.; Provencio, I.; Sollars, P.J.; Pickard, G.E. Melanopsin retinal ganglion cells receive bipolar and amacrine cell synapses. The Journal of comparative neurology 2003, 460, 380-393, doi:10.1002/cne.10652.
109. Lin, M.S.; Liao, P.Y.; Chen, H.M.; Chang, C.P.; Chen, S.K.; Chern, Y. Degeneration of ipRGCs in Mouse Models of Huntington's Disease Disrupts Non-Image-Forming Behaviors Before Motor Impairment. The Journal of neuroscience : the official journal of the Society for Neuroscience 2019, 39, 1505-1524, doi:10.1523/JNEUROSCI.0571-18.2018.
110. Aviles-Trigueros, M.; Sauve, Y.; Lund, R.D.; Vidal-Sanz, M. Selective innervation of retinorecipient brainstem nuclei by retinal ganglion cell axons regenerating through peripheral nerve grafts in adult rats. The Journal of neuroscience : the official journal of the Society for Neuroscience 2000, 20, 361-374.
111. Lindqvist, N.; Peinado-Ramonn, P.; Vidal-Sanz, M.; Hallbook, F. GDNF, Ret, GFRalpha1 and 2 in the adult rat retino-tectal system after optic nerve transection. Experimental neurology 2004, 187, 487-499, doi:10.1016/j.expneurol.2004.02.002.
112. Di Pierdomenico, J.; Garcia-Ayuso, D.; Jimenez-Lopez, M.; Agudo-Barriuso, M.; Vidal-Sanz, M.; Villegas-Perez, M.P. Different Ipsi- and Contralateral Glial Responses to Anti-VEGF and Triamcinolone Intravitreal Injections in Rats. Investigative ophthalmology & visual science 2016, 57, 3533-3544, doi:10.1167/iovs.16-19618.
113. Rovere, G.; Nadal-Nicolas, F.M.; Agudo-Barriuso, M.; Sobrado-Calvo, P.; Nieto-Lopez, L.; Nucci, C.; Villegas-Perez, M.P.; Vidal-Sanz, M. Comparison of Retinal Nerve Fiber Layer Thinning and Retinal Ganglion Cell Loss After Optic Nerve Transection in Adult Albino Rats. Investigative ophthalmology & visual science 2015, 56, 4487-4498, doi:10.1167/iovs.15-17145.
114. Ortin-Martinez, A.; Salinas-Navarro, M.; Nadal-Nicolas, F.M.; Jimenez-Lopez, M.; Valiente-Soriano, F.J.; Garcia-Ayuso, D.; Bernal-Garro, J.M.; Aviles-Trigueros, M.; Agudo-Barriuso, M.; Villegas-Perez, M.P., et al. Laser-induced ocular hypertension in adult rats does not

affect non-RGC neurons in the ganglion cell layer but results in protracted severe loss of cone-photoreceptors. Experimental eye research 2015, 132, 17-33, doi:10.1016/j.exer.2015.01.006.

115. Sanchez-Migallon, M.C.; Valiente-Soriano, F.J.; Nadal-Nicolas, F.M.; Vidal-Sanz, M.; Agudo-Barriuso, M. Apoptotic Retinal Ganglion Cell Death After Optic Nerve Transection or Crush in Mice: Delayed RGC Loss With BDNF or a Caspase 3 Inhibitor. Investigative ophthalmology & visual science 2016, 57, 81-93, doi:10.1167/iovs.15-17841.
116. Vidal-Sanz, M.; Salinas-Navarro, M.; Nadal-Nicolas, F.M.; Alarcon-Martinez, L.; Valiente-Soriano, F.J.; de Imperial, J.M.; Aviles-Trigueros, M.; Agudo-Barriuso, M.; Villegas-Perez, M.P. Understanding glaucomatous damage: anatomical and functional data from ocular hypertensive rodent retinas. Progress in retinal and eye research 2012, 31, 1-27, doi:10.1016/j.preteyeres.2011.08.001.
117. Vidal-Sanz, M.; Valiente-Soriano, F.J.; Ortin-Martinez, A.; Nadal-Nicolas, F.M.; Jimenez-Lopez, M.; Salinas-Navarro, M.; Alarcon-Martinez, L.; Garcia-Ayuso, D.; Aviles-Trigueros, M.; Agudo-Barriuso, M., et al. Retinal neurodegeneration in experimental glaucoma. Progress in brain research 2015, 220, 1-35, doi:10.1016/bs.pbr.2015.04.008.